Modular Linear Optical Circuits

PAOLO L. MENNEA[1], WILLIAM R. CLEMENTS[2], DEVIN H. SMITH[1], JAMES C. GATES[1], BENJAMIN J. METCALF[2], REX H. S. BANNERMAN[1], ROEL BURGWAL[2], JELMER J. RENEMA[2], W. STEVEN KOLTHAMMER[2,3], IAN A. WALMSLEY[2], AND PETER G. R. SMITH[1,*]

[1] *Optoelectronics Research Centre, University of Southampton, SO17 1BJ, United Kingdom*
[2] *Clarendon Laboratory, University of Oxford, Parks Rd., OX1 3PU, United Kingdom*
[3] *Department of Physics, Imperial College London, Prince Consort Rd., SW7 2BB, United Kingdom*
[*] *Corresponding author: Peter.Smith@soton.ac.uk*

Compiled August 8, 2018

Linear optical circuits that can provide reconfigurable interference between several optical modes are emerging as a powerful tool for both classical and quantum optics. In this work, we propose and demonstrate a modular architecture for building these circuits. Each module contains independent phase-controlled Mach-Zehnder interferometers, and several modules can be interfaced to build large reconfigurable interferometers. We demonstrate our approach by fabricating three modules in the form of UV-written silica-on-silicon chips. We characterize these chips, connect them to each other, and implement a wide range of linear optical transformations. Our work facilitates the development of large scale linear optical circuits for quantum optics.

OCIS codes:

http://dx.doi.org/10.1364/optica.XX.XXXXXX

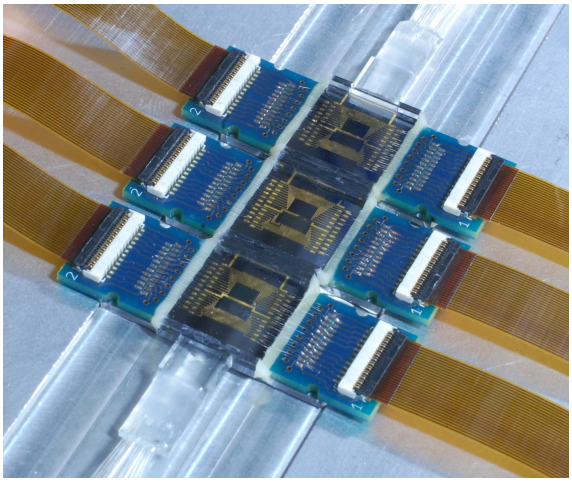

Fig. 1. Three modules of our modular, reconfigurable quantum circuits are connected to build a large and programmable multiport interferometer with 20 inputs and outputs. This three module device is glued to two fibre V-groove assemblies and the phase shifters are controlled via electrical ribbon cables. The connectivity of the interferometer is determined by the number of modules.

Integrated photonics is a promising platform for implementing the large-scale mode transformations required for optical quantum information processing [1]. Photonic chips are more compact, more stable, and easier to scale up to large sizes than alternative platforms such as bulk optics. A wide range of quantum information protocols have thus been performed on-chip, using several different materials and architectures [2–4]. In addition, large integrated interferometric circuits have applications beyond quantum information science in telecommunication and classical computing [5, 6]. To make full use of these capabilities, the development of reconfigurable integrated devices that can be used for many applications is highly desirable. In the same way that programmable electronic chips have allowed for the development of modern computing, programmable optical chips are expected to play an important role in the development of quantum optics and photonics.

However, all the devices demonstrated to date are monolithic and are designed for a fixed number of optical modes. A chip designed to manipulate a large number of modes and complex interference may not be the most appropriate for also operating on a smaller number of modes or simpler interference. Indeed, as device size increases to handle more modes, so do optical loss, optical crosstalk, and the complexity of characterizing all the optical elements on a chip. In addition, fabrication tolerances become more stringent [7, 8], since a single faulty component may jeopardize the operation of the entire device.

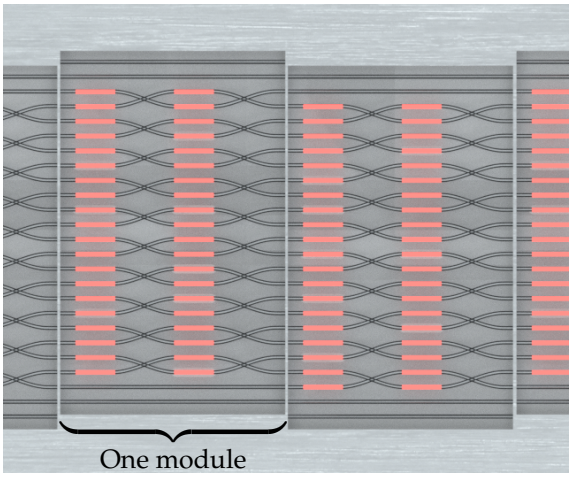

Fig. 2. A rendered impression of concatenated modular chips. The phase shifters are shown in red, and the waveguide pitch has been exaggerated for clarity. Each second chip is offset by one waveguide (127 µm) to form a multiport interferometer.

In this work, we propose and demonstrate the use of identical, flexible building blocks to compose interferometric circuits of any size. Each of these blocks consists of a column of Mach-Zehnder interferometers (MZI) with phase shifters both internally and on the input arms, as shown in fig. 1. Figure 2 illustrates how different modules may be connected to construct a large interferometric circuit. Each of these modules may be tested and characterized individually, and imperfections in the modules can be mitigated by selecting those most suitable for a given experiment. Individual chips can be added or removed depending on the desired application.

In the following sections, we present our work on designing, characterizing, and assembling modular devices for use in quantum optics experiments. We first introduce the general principles of our modular approach, and discuss design considerations for the optical components on these chips. We then describe their fabrication method and our characterization results. Finally, we assemble a three-module device and demonstrate its use by implementing a wide range of optical transformations.

1. MODULAR DESIGN

Our module consists of ten tunable MZIs placed side by side. These modules are intended to be tiled to build larger interferometers. For example, N such modules each at least $N/2$ MZI wide suffice to perform an arbitrary unitary transformation on N modes, with optimal circuit depth [9]. Here, each MZI acts as an arbitrarily reconfigurable beamsplitter, with two phase-shifters acting as the tuning elements: one internal phase setting the reflectivity and one external phase (either on the input or output) setting the phase between elements. The modules are then interlaced, as shown in fig. 2, with the left-hand outputs of one MZI fed into the right-hand inputs of the next layer of MZIs to form the N mode unitary operation with N modules.

A modular approach gives us several advantages over monolithic designs. First, it is easier in practice to work with individual layers of MZIs than it is to work with a large interferometer. Optical characterization is simpler when the modes can be addressed in small, discrete, groups. Optimizing the fabrication of a single layer of MZIs is also easier than optimizing that of an entire interferometer. Furthermore, faulty components can be replaced without compromising the entire structure.

Second, the modular approach provides experimental flexibility due to reconfigurability. Many protocols in linear optics—such as quantum teleportation [2]—do not require fully connected interferometers. For these applications, additional layers of MZIs are not necessary and merely increase loss. On the other hand, as discussed by Burgwal *et al.* [7], additional MZIs at the output of a universal multiport interferometer can be used to increase the fidelity of the overall transformation. Our modular approach allows for the addition of these MZIs if necessary. Alternatively, our approach also allows us to implement the nested-MZI architecture proposed by Miller [10] which, at the cost of additional beamsplitters, can tolerate a much higher fabrication error.

The downsides of using a modular approach are that additional coupling steps are required, and that additional loss can occur in two ways: first, there is some amount of interface loss between modules; and second, the total length of waveguide in the device is unavoidably lengthened to allow for the waveguides to match at the interfaces. However, as the waveguides are fabricated using the same process, the chips are very well mode-matched. As we show later, with the use of index-matched adhesive, we can achieve very low coupling losses.

2. COMPONENT DESIGN

A. Choice of platform

We choose UV-written silica on silicon as the platform for our modular chips. This choice is motivated by the exceptionally low coupling loss to optical fibre and propagation loss that can be achieved with this platform [11]. They are therefore compatible with many state-of-the-art photon sources and detectors that are designed to be fibre coupled. Furthermore, losses are a significant concern for quantum optics experiments and must be minimized. Moreover, UV writing does not require a lithographic step, which allows for quick turnaround times from planning to production.

B. X-couplers

We use X-couplers [12] instead of the more typical directional couplers. These X-couplers can be thought of as the zeroth-order version of a directional coupler—incoming light couples evanescently between the modes for less than one-quarter of a sine wave while transiting the device. Using these couplers instead of directional couplers has several effects: first, X-couplers are less wavelength-dependent; second, X-couplers have a compact footprint due to the small coupling region; and third, the device properties are defined primarily by the crossing angle of the two guides, improving fabrication tolerances.

C. Thermo-optic phase-shifters

The final ingredient necessary to fabricate a fully tunable device using an MZI is two phase-shifters: one inside the MZI, and one on either the input or output ports. The use of microheaters as such a phase shifter is a tried-and-tested approach in integrated quantum optics [13]. Such phase shifters have high stability and tuning range but a slow response on the order of milliseconds. Nonetheless, this response allows the device to be configured as required and remain at a fixed point during operation, which is sufficient for many protocols of interest.

In order to improve stability, *both* modes in each MZI have a phase shifter attached (see fig. 2). The total amount of current passed through the two phase-shifters is held constant, al-

lowing for push-pull operation of the phase. This increases the tuning range by a factor of two, and also ensures that the total amount of heat dissipated in each portion of the chip is constant, thus reducing cross-talk and improving stability.

3. FABRICATION

The silica glass layers are fabricated in-house by flame hydrolysis deposition (FHD) on a silicon wafer; a 15 µm thermal oxide layer forms the undercladding, onto which is deposited a 4 µm core layer doped with germanium and boron to promote photosensitivity. This is followed by an 8 µm boron and phosphorus doped upper cladding layer. Dopant levels in core and cladding are adjusted to match the refractive index to the thermal oxide.

Waveguides are directly written using a 244 nm frequency-doubled argon-ion laser into this planar structure: a focused UV beam is translated relative to the photosensitive sample on precision air-bearing stages, producing buried channel waveguides. This technique allows waveguides that are well matched to optical fibre to be produced, minimizing coupling losses. Moreover, this technique permits the inscription of programmatically-controlled Bragg gratings during the waveguide writing process, which may be written out-of-band to aid classical characterization of each module.

To enhance the refractive index change the devices are kept in a high-pressure hydrogen atmosphere for several days; however due to outgassing of the hydrogen the maximum writing time per chip is limited to about an hour. Thus, for time-limited fabrication techniques like ours a further benefit of the modular architecture is that the individual modules can be written serially, greatly increasing the number of possible devices fabricable in our laboratory.

The phase-shifters are patterned through contact lithography and lift-off of a 170 nm e-beam evaporated nichrome layer, while the wiring is a 200 nm copper layer deposited in the same manner. Computer control of the on-chip phase shifters was accomplished using custom drive electronics, producing 8 bit pulse-width-modulated drive signals at up to 20 V.

4. CHARACTERIZATION

After fabrication, the individual modules can be characterized before assembly. This characterization process is easier for our modular devices than for monolithic circuits since each MZI can be addressed individually. The emission from the two output ports of each MZI, as well as reflectance data from the Bragg gratings embedded in the waveguides before, inside, and after the MZI, yield the parameters of interest: the splitting ratios, excess loss of the couplers, an estimate of the facet loss, and the phase-shifters' tuning curves. The phase-shift of the other pair of couplers can also be found either at this stage by inputting coherent light on both inputs of an MZI or determined after the modules are assembled.

Table 1 shows typical values for the parameters of interest measured this way for the chips used here, which can be compared to the state of the art [4]. Fiber to chip coupling losses and propagation losses are similar to what has been demonstrated with recent on-chip quantum experiments [2, 3], but could still be improved. Chip to chip coupling losses are low, as expected. However, the coupler excess loss is particularly high, and the coupler splitting ratios are different from the 50% that is required to construct fully tunable MZIs. This is due to thermal effects during metal deposition, which were neglected during design and can be compensated for (see Supplement 1).

Table 1. Typical measured parameters of interest for fabricated modular chips, as determined from module characterization, at an operating wavelength of 780 nm. For experimental details, please see sections 1-3 of Supplement 1.

Fibre coupling loss	0.8 ± 0.1 dB
Chip-to-chip coupling loss	0.2 ± 0.1 dB
Propagation loss	0.35 ± 0.04 dB cm^{-1}
Coupler excess loss	2.1 ± 0.3 dB
Phase tuning range	$(2.7\pm0.2)\pi$rad
Coupling ratio (transmittivity)	$57\pm4\%$

We also find that our thermal crosstalk measurements justify the use of our dual heater design. To measure crosstalk, a MZI is placed close to its 50:50 point and its outputs measured as settings of adjacent heaters were varied. This is carried out both in the case of complementary heating and with one heater in each pair disabled. We find that when achieving a π phase shift on the target MZI, our dual heaters induce a crosstalk of about 0.01π to the neighboring MZI and of 0.007π to the next-nearest MZI, whereas using a single phase shifter to achieve the same phase shift induces about twice as much crosstalk.

5. EXPERIMENTAL RESULTS

To perform a demonstration of these devices, we assemble three modular chips using two six-axis stages with sub-micron precision. We then show that the resulting assembly, shown in fig. 1, can implement a wide range of useful optical transformations.

As a first demonstration of our three chip assembly, we show that light from one input can be switched to any of its six available outputs. The procedure for doing so is straightforward. We send light into the input, monitor the output that we seek to switch the light into, and sequentially optimize the MZIs on each chip along the path to that output to maximize the measured power. Our results are shown in Fig. 3 (b). We see that our chip assembly successfully routes most of the light to the desired output, for all six outputs. However, some leakage does occur, which may originate from both the imperfect splitting ratios of the beam splitters and some light recoupling into the waveguides after being lost.

Next, we show that our chip assembly can implement a balanced 3×3 interferometer, also known as a tritter. Tritters can be used for fundamental studies of quantum interference [14], as well as for classical photonics applications. We use a self-configuring approach to implement a tritter [10], which does not require detailed prior characterization of the phase shifters. Our results are shown in fig. 3 (d). We see that the light is indeed equally split between all output ports.

More generally, we also demonstrate that our chip assembly implements a 3×3 universal multiport interferometer [9]: a device that can realize any linear transformation between 3 input and output optical channels. We first fully characterize the 2×2 transformations implemented by the relevant MZIs and phase shifters for all of their phase shifter settings using an automated procedure. We then randomly select a 3×3 unitary matrix U to be implemented with our device. We perform a decomposition procedure on U that yields the correct phase shifter settings [9], which we program into our device. To test the performance of this protocol, we then measure the 3×3 transfer matrices corresponding to all 9 input-output relations, which we normalize

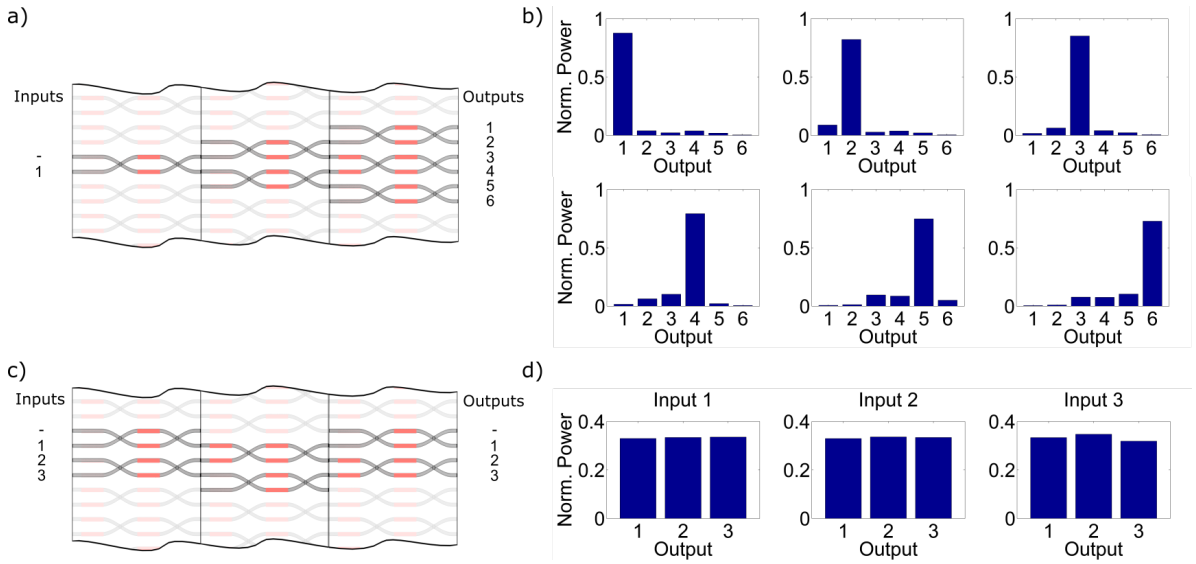

Fig. 3. Experimental results demonstrating the programmability of our three chip device. a) Our device can be configured to act as a 1×6 switch. The six relevant phase shifter pairs that we use to program the switch are schematically represented by red bars in the circuit. b) Bar plots of the output intensities when the device is configured to switch the light towards a given output, for all six possible outputs. c) Our device can also be configured to act as a balanced 3 × 3 interferometer (a tritter) using the four phase shifter pairs shown in this circuit. d) Bar plots of the output intensities for all three inputs when the device is configured as a tritter. For experimental details, please see sections 4 and 5 of Supplement 1.

to remove the effect of loss. We repeat this process for 50 randomly selected unitary matrices and experimentally measure the transfer matrices for all of them. We compare these transfer matrices to the targeted transformations and find an average transformation fidelity of 97.5%, which confirms that our circuits operate as intended and provide similar capabilities to other state-of-the-art integrated linear optical platforms [3, 4, 6].

6. CONCLUSION

We have designed and fabricated a modular system for implementing interferometers of arbitrary size. Our modular architecture is platform independent and provides a route to building large and adaptable interferometers that are tolerant to fabrication errors and easy to characterize. In addition, our particular implementation of the modular system is fabricated with fiber-compatible silica waveguides, reducing loss both at the internal and external interfaces to quantum-compatible tolerances; we additionally used push-pull phase-shifters, which substantially reduce crosstalk between neighboring devices. Going forward, these devices will be used to implement a wide range of quantum interferometric protocols with smooth scaling in size.

Data associated with this work are available from [15]. See Supplement 1 for supporting content.

Funding Engineering and Physical Sciences Research Council (EPSRC) (EP/K034480/1 and EP/M013243/1), European Commission (H2020-FETPROACT-2014 grant QUCHIP). J.J.R. acknowledges support from NWO Rubicon.

REFERENCES

1. J. L. O'Brien, A. Furusawa, and J. Vučković, Nat. Photonics **3**, 687 (2009).
2. B. J. Metcalf, J. B. Spring, P. C. Humphreys, N. Thomas-Peter, M. Barbieri, W. S. Kolthammer, X.-M. Jin, N. K. Langford, D. Kundys, J. C. Gates, B. J. Smith, P. G. R. Smith, and I. A. Walmsley, Nat. Photonics **8**, 770 (2014).
3. J. Carolan, C. Harrold, C. Sparrow, E. Martín-López, N. J. Russell, J. W. Silverstone, P. J. Shadbolt, N. Matsuda, M. Oguma, M. Itoh, G. D. Marshall, M. G. Thompson, J. C. F. Matthews, T. Hashimoto, J. L. O'Brien, and A. Laing, Science **349**, 711 (2015).
4. F. Flamini, N. Spagnolo, and F. Sciarrino, arXiv preprint arXiv:1803.02790 (2018).
5. J. Capmany, I. Gasulla, and D. Pérez, Nat. Photonics **10**, 6 (2016).
6. Y. Shen, N. C. Harris, S. Skirlo, M. Prabhu, T. Baehr-Jones, M. Hochberg, X. Sun, S. Zhao, H. Larochelle, D. Englund, and M. Soljačić, Nat. Photonics **11**, 441 (2017).
7. R. Burgwal, W. R. Clements, D. H. Smith, J. C. Gates, W. S. Kolthammer, J. J. Renema, and I. A. Walmsley, Opt. Express **25**, 28236 (2017).
8. N. J. Russell, L. Chakhmakhchyan, J. L. OBrien, and A. Laing, New J. Phys. **19**, 033007 (2017).
9. W. R. Clements, P. C. Humphreys, B. J. Metcalf, W. S. Kolthammer, and I. A. Walmsley, Optica. **3**, 1460 (2016).
10. D. A. B. Miller, Optica. **2**, 747 (2015).
11. D. Zauner, K. Kulstad, J. Rathje, and M. Svalgaard, Electron. Lett. **34**, 1582 (1998).
12. D. O. Kundys, J. C. Gates, S. Dasgupta, C. B. E. Gawith, and P. G. R. Smith, IEEE Photonics Technol. Lett. **21**, 947 (2009).
13. B. J. Smith, D. Kundys, N. Thomas Peter, and I. A. Walmsley, Opt. Express **17**, 264 (2009).
14. A. J. Menssen, A. E. Jones, B. J. Metcalf, M. C. Tichy, S. Barz, W. S. Kolthammer, and I. A. Walmsley, Phys. Rev. Lett. **118**, 153603 (2017).
15. P. Mennea (2018). https://doi.org/10.5258/SOTON/D0474.

FULL REFERENCES

1. J. L. O'Brien, A. Furusawa, and J. Vučković, "Photonic quantum technologies," Nat. Photonics **3**, 687 (2009).
2. B. J. Metcalf, J. B. Spring, P. C. Humphreys, N. Thomas-Peter, M. Barbieri, W. S. Kolthammer, X.-M. Jin, N. K. Langford, D. Kundys, J. C. Gates, B. J. Smith, P. G. R. Smith, and I. A. Walmsley, "Quantum teleportation on a photonic chip," Nat. Photonics **8**, 770–774 (2014).
3. J. Carolan, C. Harrold, C. Sparrow, E. Martín-López, N. J. Russell, J. W. Silverstone, P. J. Shadbolt, N. Matsuda, M. Oguma, M. Itoh, G. D. Marshall, M. G. Thompson, J. C. F. Matthews, T. Hashimoto, J. L. O'Brien, and A. Laing, "Universal linear optics," Science **349**, 711–716 (2015).
4. F. Flamini, N. Spagnolo, and F. Sciarrino, "Photonic quantum information processing: a review," arXiv preprint arXiv:1803.02790 (2018).
5. J. Capmany, I. Gasulla, and D. Pérez, "Microwave photonics: The programmable processor," Nat. Photonics **10**, 6 (2016).
6. Y. Shen, N. C. Harris, S. Skirlo, M. Prabhu, T. Baehr-Jones, M. Hochberg, X. Sun, S. Zhao, H. Larochelle, D. Englund, and M. Soljačić, "Deep learning with coherent nanophotonic circuits," Nat. Photonics **11**, 441 (2017).
7. R. Burgwal, W. R. Clements, D. H. Smith, J. C. Gates, W. S. Kolthammer, J. J. Renema, and I. A. Walmsley, "Using an imperfect photonic network to implement random unitaries," Opt. Express **25**, 28236–28245 (2017).
8. N. J. Russell, L. Chakhmakhchyan, J. L. OBrien, and A. Laing, "Direct dialling of haar random unitary matrices," New J. Phys. **19**, 033007 (2017).
9. W. R. Clements, P. C. Humphreys, B. J. Metcalf, W. S. Kolthammer, and I. A. Walmsley, "Optimal design for universal multiport interferometers," Optica. **3**, 1460–1465 (2016).
10. D. A. B. Miller, "Perfect optics with imperfect components," Optica. **2**, 747–750 (2015).
11. D. Zauner, K. Kulstad, J. Rathje, and M. Svalgaard, "Directly UV-written silica-on-silicon planar waveguides with low insertion loss," Electron. Lett. **34**, 1582–1584 (1998).
12. D. O. Kundys, J. C. Gates, S. Dasgupta, C. B. E. Gawith, and P. G. R. Smith, "Use of cross-couplers to decrease size of uv written photonic circuits," IEEE Photonics Technol. Lett. **21**, 947–949 (2009).
13. B. J. Smith, D. Kundys, N. Thomas Peter, and I. A. Walmsley, "Phase-controlled integrated photonic quantum circuits," Opt. Express **17**, 264–267 (2009).
14. A. J. Menssen, A. E. Jones, B. J. Metcalf, M. C. Tichy, S. Barz, W. S. Kolthammer, and I. A. Walmsley, "Distinguishability and many-particle interference," Phys. Rev. Lett. **118**, 153603 (2017).
15. P. Mennea (2018). https://doi.org/10.5258/SOTON/D0474.